PACS numbers: 42.25.Ja; 42.25.Lc; 42.79.Ci
DOI: 10.1070/QE2002v032n01ABEH002134

The use of crystalline quartz for compensation for thermally induced depolarisation in Faraday isolators

N.F.Andreev, E.V.Katin, O.V.Palashov, A.K.Potemkin, D.H.Reitze, A.M.Sergeev, E.A.Khazanov

***Abstract*. It is shown that a quartz crystal, which is placed inside a telescope and whose optic axis is parallel to a light beam, can reduce the depolarisation of radiation caused by thermally induced birefringence in a Faraday isolator. The isolation ratio was experimentally increased by a factor of eight. An important advantage of this method over previous methods is that standard commercial Faraday rotators can be used.**

Keywords: *Faraday isolator, high-average power lasers, thermally induced birefringence, depolarisation.*

1. Introduction

Thermal effects caused by absorption of laser radiation in Faraday isolators [1 – 6] are one of the factors preventing the development and use of high-power single-mode solid-state lasers. Many applications (see, for example, [7, 8]) require a combination of the high average radiation power with a low non-isolation of a Faraday isolator, i.e., with a high isolation ratio. Thermal effects resulting in the depolarisation of laser radiation and, hence, reducing the isolation ratio, namely, the temperature dependence of the Verdet constant and the photoelasticity have been studied for the first time in papers [9 – 12]. In paper [10], it was predicted theoretically that the photoelasticity effect limits the isolation ratio at high average powers, whereas the temperature dependence of the Verdet constant can be neglected. This conclusion was confirmed experimentally in papers [11, 13, 14].

In paper [10], the quality parameter was determined which characterises a magnetically active medium from the point of view of minimisation of the non-isolation at high average radiation powers. This parameter was measured for a terbium gallium garnet (TGG) crystal and some magnetically active glasses in papers [15, 16]. The dependence of the Faraday-isolator non-isolation on the orientation of a magnetically active crystal was studied in detail in paper [15].

In paper [12], two new schemes of a Faraday isolator were proposed and theoretically studied which provide a partial compensation for self-induced depolarisation in a magnetically active medium. The schemes contain three optical elements: two Faraday rotators, each of them rotating the polarisation plane through 22.5°, and a reciprocal optical element placed between them. The experiments [13, 14] confirmed the high efficiency of these schemes.

However, the use of two Faraday rotators is not always convenient and results in an increase in the Faraday-isolator size. In addition, it is virtually impossible to employ standard commercial Faraday isolators in this case because the magnetic system and optical elements should be substantially rearranged. In this paper, we proposed and experimentally implemented a new method of compensating for depolarisation in a Faraday isolator, which allows the use of standard 45° Faraday rotators in high-power laser systems.

2. Increasing the isolation ratio with the help of a quartz rotator

Our method of compensation for depolarisation in a Faraday isolator is based on the use of a phase plate capable of subtracting all phase incursions acquired by a light beam in the Faraday element. Such a phase plate should have the same transverse distribution of eigen polarisations as the Faraday rotator and should have the same transverse distribution of the phase difference, but only with the opposite sign. In this case, radiation propagated successively through two such phase plates will retain its initial polarisation. The nonreciprocal properties of the Faraday isolator (rotation of polarisation through 90° after two transits) are also retained.

In the presence of the temperature gradient, a superposition of two types of birefringence takes place in the Faraday element: circular birefringence (Faraday effect) and linear birefringence (photoelastic effect). Circular birefringence is characterised by the phase incursion δ_c, which is independent of polar coordinates r and φ because we neglect the temperature dependence of the Verdet constant. Linear birefringence is characterised by the phase incursion δ_{lin} and by the tilt angle of eigen polarisations. In a cylindrical element made of glass or a cubic crystal with the orientation [111], the value of δ_{lin} is independent of φ and is proportional to r^2 near the beam axis, while eigen polarisations are directed along the radial and tangential directions, i.e., their

N.F.Andreev, E.V.Katin, O.V.Palashov, A.K.Potemkin, A.M.Sergeev, E.A.Khazanov Institute of Applied Physics, Russian Academy of Sciences, ul. Ul'yanova 46, 603600 Nizhnii Novgorod, Russia; www.sci-nnov.ru/science/science/appl.new
D.H.Reitze NFB, University of Florida, Physical Department, Gainesville, FL 32611, USA; www.ufl.edu

Received 13 August 2001
Kvantovaya Elektronika **32** (1) 91 – 94 (2002)
Translated by M.N.Sapozhnikov

tilt angle equals φ. (This is not the case when crystals with other orientations are used [15, 17]; however, we will not consider these cases.) Due to the superposition of the two types of birefringence, the eigen polarisations of the Faraday element become elliptical, the tilt angle of the axis of the ellipse being φ, while the ellipticity and the phase difference being dependent only on r.

It is known that the superposition of linear and circular birefringence also takes place upon the propagation of a plane wave in crystalline quarts at an angle of θ to the optic axis. The phase incursion $\delta_{\mathrm{q\,lin}}$ for linear birefringence depends quadratically on θ for $\theta \ll 1$, whereas the phase difference for $\delta_{\mathrm{q\,c}}$ circular birefringence weakly depends on θ for $\theta \ll 1$.

Upon the propagation of a converging or diverging beam (Fig. 1), the tilt angle of the eigen polarisation of linear birefringence equals φ, while the angle θ is proportional to r, i.e., $\delta_{\mathrm{q\,lin}} \sim r^2$. Therefore, the distributions of the ellipticity of eigen polarisations and of the phase shift between them in the Faraday element and a quartz crystal are close to each other, while the tilt angles of the ellipse exactly coincide. If the directions of polarisation rotation in the Faraday element and quartz are opposite (i.e., δ_{c} and $\delta_{\mathrm{q\,c}}$ have opposite signs), depolarisation can be compensated after the successive propagation of the light beam through the Faraday element and the quartz crystal.

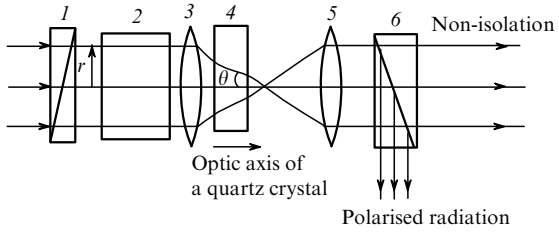

Figure 1. Scheme for compensation for depolarisation in a Faraday isolator: (*1*, *6*) crossed polarisers; (*2*) 45° Faraday rotator; (*3*, *5*) telescope lenses; (*4*) 45° quartz rotator; (θ) angle between the wave vector and the optic axis of a quartz crystal; (r) polar radius.

Let us find conditions for the most efficient compensation. Because the laser beam simultaneously records distortions (being a thermal source) and reads them, the self-action depends on the transverse intensity distribution, in particular, on the rate of its decrease from the centre to periphery [18]. The compensation efficiency also can depend substantially on the beam shape because the dependence $\delta_{\mathrm{lin}}(r)$ is completely determined by the intensity distribution.

Consider a super-Gaussian beam with the radius r_0:

$$\boldsymbol{E}_{\mathrm{in}} = E_0 \boldsymbol{x}_0 \exp\left(-\frac{r^{2m}}{2r_0^{2m}}\right), \tag{1}$$

where $\boldsymbol{x}_0$ is the unit vector along the x axis and the parameter m characterises the rate of the intensity fall. For $m = 1$, the intensity falls rather slowly (a Gaussian beam). As m increases, the rate of the intensity fall increases, and for $m \to \infty$ the beam shape tends to rectangular.

The Jones matrices for the Faraday rotator (F) and quartz (R_{q}) have the form [10, 19, 20]

$$F = \sin\frac{\delta}{2}\begin{pmatrix} \cot\dfrac{\delta}{2} - \mathrm{i}\dfrac{\delta_{\mathrm{lin}}}{\delta}\cos 2\varphi & -\dfrac{\delta_{\mathrm{c}}}{\delta} - \mathrm{i}\dfrac{\delta_{\mathrm{lin}}}{\delta}\sin 2\varphi \\ \dfrac{\delta_{\mathrm{c}}}{\delta} - \mathrm{i}\dfrac{\delta_{\mathrm{lin}}}{\delta}\sin 2\varphi & \cot\dfrac{\delta}{2} + \mathrm{i}\dfrac{\delta_{\mathrm{lin}}}{\delta}\cos 2\varphi \end{pmatrix}, \tag{2}$$

$$R_{\mathrm{q}} = \sin\frac{\delta_{\mathrm{q}}}{2}\begin{pmatrix} \cot\dfrac{\delta_{\mathrm{q}}}{2} - \mathrm{i}\dfrac{\delta_{\mathrm{q\,lin}}}{\delta_{\mathrm{q}}}\cos 2\varphi & -\dfrac{\delta_{\mathrm{q\,c}}}{\delta_{\mathrm{q}}} - \mathrm{i}\dfrac{\delta_{\mathrm{q\,lin}}}{\delta_{\mathrm{q}}}\sin 2\varphi \\ \dfrac{\delta_{\mathrm{q\,c}}}{\delta_{\mathrm{q}}} - \mathrm{i}\dfrac{\delta_{\mathrm{q\,lin}}}{\delta_{\mathrm{q}}}\sin 2\varphi & \cot\dfrac{\delta_{\mathrm{q}}}{2} + \mathrm{i}\dfrac{\delta_{\mathrm{q\,lin}}}{\delta_{\mathrm{q}}}\cos 2\varphi \end{pmatrix}, \tag{3}$$

where

$$\delta^2 = \delta_{\mathrm{lin}}^2 + \delta_{\mathrm{c}}^2;\ \delta_{\mathrm{q}}^2 = \delta_{\mathrm{q\,lin}}^2 + \delta_{\mathrm{q\,c}}^2;\ \delta_{\mathrm{c}} = \frac{\pi}{2};\ \delta_{\mathrm{q\,c}} = -\frac{\pi}{2};$$

$$\delta_{\mathrm{lin}} = \frac{1+2\xi}{3}\frac{p}{\sigma_0}\frac{f(y)}{y};\ \delta_{\mathrm{q\,lin}} = p_{\mathrm{q}} y;$$

$$f(y) = \int_0^y \left(\int_0^z \exp\left(-x^m\right)\mathrm{d}x\right)\mathrm{d}z;\ \sigma_0 = \int_0^\infty \exp\left(-y^m\right)\mathrm{d}y;$$

$$y = \frac{r^2}{r_0^2};\ p = \frac{\alpha Q}{\kappa}\frac{LP_0}{\lambda};\ p_{\mathrm{q}} = \frac{\pi}{2}\frac{n_{\mathrm{o}} - n_{\mathrm{e}}}{|\Delta n_{\mathrm{c}}|}\frac{r_0^2}{n^2 f^2};$$

$$\xi = \frac{2p_{44}}{p_{11} - p_{12}};\ Q = \left(\frac{1}{L}\frac{\mathrm{d}L}{\mathrm{d}T}\right)\frac{n^3}{4}\frac{1+v}{1-v}(p_{11} - p_{12}).$$

Here, L, $(1/L)\mathrm{d}L/\mathrm{d}T$, v, κ, n, p_{ij} are the length, the thermal expansion coefficient, Poisson's ratio, the thermal conductivity, the refractive index, and the photoelasticity coefficients for a magnetically active medium in the two-index notation [21], respectively; T is the temperature; λ is the wavelength in vacuum; P_0 is the radiation power; n_{o} and n_{e} are the refractive indices for the ordinary and extraordinary waves in quartz; $n = (n_{\mathrm{o}} + n_{\mathrm{e}})/2$; Δn_{c} is the difference of refractive indices for the right-hand and left-hand polarised waves in quartz for $\theta = 0$; and f is the focal length of lens (*3*). We neglected the temperature dependence of the Verdet constant and took into account that δ_{c} and $\delta_{\mathrm{q\,c}}$ have opposite signs (see above). In addition, we took into account that $\theta = r/(nf)$ in the paraxial approximation.

If the beam that has passed through polariser (*1*) (see Fig. 1) is described by expression (1), then the beam incident on polariser (*6*) is determined by the expression

$$\boldsymbol{E}_{\mathrm{out}} = FR_{\mathrm{q}}\boldsymbol{E}_{\mathrm{in}}. \tag{4}$$

Hereafter, we assume that the transit from polariser (*1*) to polariser (*6*) is a backward transit of radiation through the Faraday isolator, for example, from amplifiers to a master oscillator. Therefore, in the case of an ideal isolation, all radiation should be reflected by polariser (*6*) and no radiation should pass through polariser (*6*) to the master oscillator.

The non-isolation γ (the ratio of the radiation power transmitted by polariser (*6*) to the output power) is determined by the expression

$$\gamma = \frac{\displaystyle\int_0^{2\pi}\int_0^\infty |\boldsymbol{E}_{\mathrm{out}}\boldsymbol{y}_0|^2 r\mathrm{d}r\mathrm{d}\varphi}{\displaystyle\int_0^{2\pi}\int_0^\infty |\boldsymbol{E}_{\mathrm{out}}|^2 r\mathrm{d}r\mathrm{d}\varphi}. \tag{5}$$

Hereafter, we will neglect the aperture losses and will integrate over r in (5) up to infinity.

Consider first the case of weak linear birefringence in a Faraday element

$$\delta_{\rm lin} \ll 1. \tag{6}$$

Because $\delta_{\rm q\,lin}$ should be close to $\delta_{\rm lin}$ to obtain the efficient compensation, we will assume that $\delta_{\rm q\,lin} \ll 1$. In this case, by substituting (1)–(4) into (5) and integrating, taking into account (6), we obtain

$$\gamma = \frac{1}{\pi^2}\left\{\frac{\sigma_2}{\sigma_0}p_{\rm q}^2 + 2\frac{1+2\xi}{3}p_{\rm q}p\left[\frac{\sigma_2}{\sigma_0}A_0(m)\right]^{1/2} + \left(\frac{1+2\xi}{3}\right)^2 p^2 A_1(m)\right\}, \tag{7}$$

where

$$A_0(m) = \frac{1}{\sigma_2\sigma_0^3}\left[\int_0^\infty f(y)\exp(-y^m)\mathrm{d}y\right]^2;$$

$$A_1(m) = \frac{1}{\sigma_0^3}\int_0^\infty \frac{f^2(y)}{y^2\exp(y^m)}\mathrm{d}y; \quad \sigma_2 = \int_0^\infty y^2\exp(-y^m)\mathrm{d}y.$$

For $p_{\rm q} = 0$, we obtain from (7) the known expression for the non-isolation $\gamma_{\rm old}$ in the traditional scheme of a Faraday isolator [12, 18]

$$\gamma_{\rm old} = \left(\frac{1+2\xi}{3}\right)^2\frac{p^2}{\pi^2}A_1(m). \tag{8}$$

One can see from (7) that γ depends on two dimensionless parameters: the normalised radiation power p and the normalised birefringence $p_{\rm q}$ in quartz. Note that $p_{\rm q}$ depends quadratically on the beam convergence angle r_o/f.

One can see from (7) and (8) that the compensation of depolarisation is possible only when $p_{\rm q}$ and p have opposite signs because otherwise $\gamma > \gamma_{\rm old}$ for any $p_{\rm q}$. Physically, this is explained by the fact that the phase incursions in Faraday rotator $\delta_{\rm lin}$ and quartz $\delta_{\rm q\,lin}$ should have opposite signs. Because $n_{\rm o} > n_{\rm e}$ in quartz, we have $p_{\rm q} > 0$. The sign of p is determined by the sign of Q. We determined the signs of Q for a magnetically active MOS-115-35 glass and a TGG crystal using the method described in paper [22]. In both cases, $Q < 0$, which shows that the compensation can be achieved by the method proposed. Note that when $Q > 0$, this method also can be used by placing an additional 90° polarisation rotator between Faraday rotator (*2*) and lens (*3*). The calculation shows that this will result in a change of the sign plus to minus in front of the second term in expression (7).

By differentiating γ with respect to $p_{\rm q}$ and equating the derivative to zero, we obtain the optimal value of $p_{\rm q\,opt}$ and the minimal non-isolation

$$\gamma_{\rm min} = \left(\frac{1+2\xi}{3}\right)^2\frac{p^2}{\pi^2}[A_1(m) - A_0(m)]. \tag{9}$$

3. Experimental results and discussion

We used in the experiment (Fig. 1) linearly polarised radiation from a cw Nd : YLF laser (Photonics Industries) with the transverse intensity distribution close to Gaussian, which corresponds to $m = 1$. Iceland calcite wedges were used as polarisers. We also used a commercial Faraday rotator (with the rotation angle 45°) based on a TGG crystal. The non-isolation was determined using power-meters. By changing the distance between telescope lenses, we could compensate the thermal lens of the Faraday rotator. Note also that we can use a telescope consisting of the positive and negative lenses, which allows us to reduce its length down to 1 cm. The experiments were performed in two geometries with the focal lengths of lenses $f = 88$ and 125 mm. For each geometry, the dependence of γ on the radiation power was measured.

Fig. 2 shows the experimental dependences $\gamma_{\rm old}(P_0)$ and $\gamma(P_0)$ for the two above values of f. Thermal effects are weak at low powers, and $\gamma_{\rm old}$ is determined by 'cold' birefringence in the medium, while γ is determined only by the value of $p_{\rm q}$. In this case, $\gamma(P_0 \to 0) > \gamma_{\rm old}(P_0 \to 0)$, i.e., the traditional scheme provides a better isolation at low powers. Note that the Faraday isolator proposed in papers [10–12] does not have this drawback. When power is increased up to the optimal value $P_{\rm opt}$, depolarisation γ decreases and reaches the minimum. As P_0 is further increased, the non-isolation γ begins to grow.

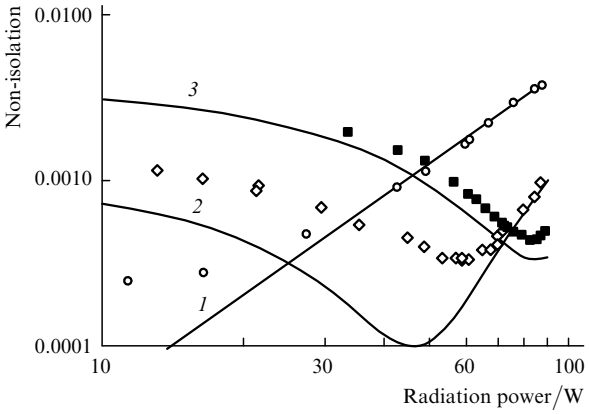

Figure 2. Non-isolation $\gamma_{\rm old}(P_0)$ of the traditional Faraday-isolator scheme (*1*, circles) and non-isolation $\gamma(P_0)$ with a quartz compensator for $f = 125$ (*2*, rhombs) and 88 mm (*3*, squares). Theoretical dependences are plotted by expressions (7) and (8).

Fig. 2 also shows the theoretical dependences $\gamma_{\rm old}(P_0)$ and $\gamma(P_0)$ plotted by expressions (7) and (8). The product $Q\alpha$ for a TGG crystal was measured by the method described in papers [15, 16]. Without compensation (curve *1*, Fig. 2), the theory well agrees with the experiment at high powers when the thermally induced non-isolation is far greater than the 'cold' non-isolation $\gamma_{\rm cool} = 2.5 \times 10^{-4}$. For $f = 125$ mm, the experimental value of $\gamma_{\rm min}$ is substantially greater than the theoretical value. This is explained by the influence of the 'cold' non-isolation, which exceeds the theoretical value of $\gamma_{\rm min}$ by a factor of 2.5 in this case.

The excess of the experimental value of $P_{\rm opt}$ over its theoretical value is probably explained by the same reason. At high powers, the influence of 'cold' depolarisation is negligible ($\gamma_{\rm cool} \ll \gamma$), and the theoretical and experimental values of γ coincide. For $f = 88$ mm (curve *3*), the experimental value of $P_{\rm opt}$ well agrees with the theoretical value. The experimental values of γ are somewhat greater than theoretical values, but the difference is not great.

The ratio $G_{\rm max} = \gamma_{\rm old}/\gamma_{\rm min}$ is the most important from the practical point of view. It shows how much the isolation ratio can be increased by using the method proposed here.

We obtain from (8) and (9)

$$G_{\max}(m) = \frac{A_1(m)}{A_1(m) - A_0(m)}. \quad (10)$$

Table 1 presents the values of A_0, A_1 and $G_{\max}$ for different m. One can see that the compensation efficiency increases substantially with increasing m, which can be simply explained as follows. The higher m, the closer the beam profile to the rectangular one and, hence, the closer the temperature distribution to a parabolic distribution. The quantity δ_{lin} is proportional to r^2 only for a parabolic distribution of temperature [18]. In this case, for the optimal value of p_q, we have $\delta_{\text{lin}} = -\delta_{q\,\text{lin}}$ at any point of the beam cross section and depolarisation is completely compensated: $G_{\max} \to \infty$. We obtained the experimental value $G_{\max} = 8$ instead of the theoretical value $G_{\max}(m=1)=11.5$. This difference is caused by the beam ellipticity and by the fact that lens (*3*) and the laser beam are not perfectly coaxial.

Table 1. Values of A_0, A_1, and $G_{\max}$ for different m.

m	A_0	A_1	$G_{\max}$
1	1/8	0.137	11.5
2	0.109	0.111	66.7
4	0.095	0.095	640
8	0.087	0.087	9650
16	0.085	0.085	200000
∞	1/12	1/12	∞

The value of $G_{\max}$ is independent of the radiation power [see expression (10)] only when the condition (6) is satisfied. In the general case, the numerical integration of (5) taking into account expressions (1)–(4) shows that the value of $G_{\max}$ decreases with increasing parameter p (Fig. 3). This is explained by the saturation of the dependence $\gamma_{\text{old}}(p)$ for $p \sim 1$ because depolarisation decreases with increasing δ_{lin} from π to 2π [11, 12]. The latter circumstance also concerns $\delta_{q\,\text{lin}}$, but the difference of the dependence $\delta_{\text{lin}}(r)$ from a parabola increases with increasing p, and, hence, $G_{\max}$ decreases. For a rectangular beam profile ($m = \infty$), $\gamma_{\min} = 0$ for any δ_{lin}.

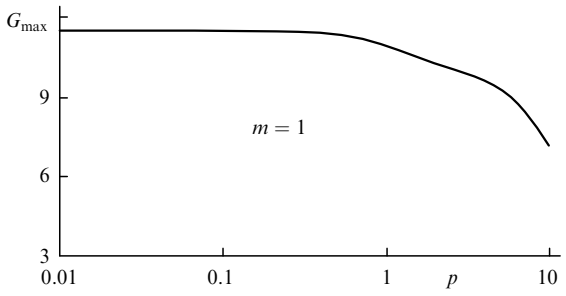

Figure 3. Dependence of the increase in the isolation ratio $G_{\max}$ on the normalised power p for $m = 1$.

4. Conclusions

The efficiency of the method for compensation and depolarisation of a Faraday isolator substantially depends on the beam profile, being maximal for a rectangular beam and minimal for a Gaussian beam. In the latter case, the isolation ratio increases by an order of magnitude for $p < 2$, which corresponds to the radiation power $P_0 < 1$ kW for a TGG crystal [15] and $P_0 < 200$ W for glass [16]. An important advantage of this method over the methods considered in papers [12–14] is the possibility of using standard commercial Faraday rotators with the rotation angle 45°.

Note also that the use of a non-gyrotropic uniaxial crystal instead of a quartz crystal allows the compensation for depolarisation in active elements of lasers [23].

Acknowledgements. This work was supported by the NSF Grant PHY-9900786 (USA) and by the Russian Foundation for Basic Research (Grant No. 99-02-17257).

References

1. Andreev N.F., Palashov O.V., Pasmanik G.A., Khazanov E.A. Khazanov E.A. *Kvantovaya Electron.,* **24**, 581 (1997) [*Quantum Electron*., **27**, 565 (1997)].
2. Andreev N., Khazanov E., Kulagin O., Movshevich B., Palashov O., Pasmanik G., Rodchenkov V., Scott A., Soan P. *IEEE J. Quantum Electron*., **35**, 110 (1999).
3. Eichler H.J., Mehl O., Eichler J. *Proc. SPIE Int. Opt. Soc. Eng*., **3613**, 166 (1999).
4. Lai K.S., Wu R., Phua P.B. *Proc. SPIE Int. Opt. Soc. Eng*., **3928**, 43 (2000).
5. Hirano Y., Yamamoto S., Tajime T., Taniguchi H., Nakamura M. *Proc. CLEO'2000. Postdeadline papers (OSA Technical Digest)* (Optical Society of America, Washington DC, 2000), p. 13–14.
6. Khazanov E.A. *Kvantovaya Electron*., **31**, 351 (2001) [*Quantum Electron*., **31**, 351 (2001)].
7. Abramovici A., Althouse W.E., Drever R.W.P., et al. *Science*, **256**, 325 (1992).
8. Kanabe T., Kawashima T., Matsui H., Okada Y., Kawada Y., Eguchi T., Kandasamy R., Kato Y., Terada M., Yamanaka M., Nakatsuka M., Izawa Y., Nakai S., Kanzaki T., Miyajima H., Miyamoto M., Kan H. *Proc. SPIE Int. Opt. Soc. Eng*., **3889**, 190 (2000).
9. Khazanov E.A., Kulagin O.V., Yoshida S., Reitze D. *Proc. CLEO'98* (OSA Technical Digest) (Optical Society of America, Washington DC, 1998), p. 250–251.
10. Khazanov E.A., Kulagin O.V., Yoshida S., Tanner D., Reitze D. *IEEE J. Quantum Electron*., **35**, 1116 (1999).
11. Khazanov E.A. *Proc. SPIE Int. Opt. Soc. Eng*., **3609**, 181 (1999).
12. Khazanov E.A. *Kvantovaya Electron*., **26**, 59 (1999) [*Quantum Electron*., **29**, 59 (1999)].
13. Khazanov E., Andreev N., Babin A., Kiselev A., Palashov O., Reitze D. *J. Opt. Soc. Am. B*, **17**, 99 (2000).
14. Andreev N.F., Palashov O.V., Potemkin A.K., Reitze D.H., Sergeev A.M., Khazanov E.A. *Kvantovaya Electron*., **30**, 1107 (2000) [*Quantum Electron.,* **30**, 1107 (2000)].
15. Khazanov E., Andreev N., Palashov O., Poteomkin A., Sergeev A., Mehl O., Reitze D. *Appl. Opt.* (to be published).
16. Andreev N.F., Babin A.A., Zarubina T.V., Kisilev A.M., Palasov O.V., Khazanov E.A. Shchavelev O.S. *Optich. Zh*., **67**, 66 (2000).
17. Soms L.N., Tarasov A.A. *Kvantovaya Electron*., **6**, 2546 (1979) [*Sov. J. Quantum Electron*., **9**, 1506 (1979)].
18. Khazanov E.A. *Kvantovaya Electron*., **30**, 147 (2000) [*Quantum Electron*., **30**, 147 (2000)].
19. Tabor M.J., Chen F.S. *Appl. Phys*., **40**, 2760 (1969).
20. Jaecklin A.A., Lietz M. *Appl. Opt.,* **11**, 617 (1972).
21. Nye J.F. *Physical Properties of Crystals: Their Representation by Tensors and Matrices* (Oxford: Clarendon Press, 1957).
22. Born M., Wolf E. *Principles of Optics* (Oxford: Pergamon Press, 1969).
23. Khazanov E.A., Katin E.V., Poteomkin A.K. *J. Opt. Soc. Am. B*, **19** (2) (2002).